Measuring Small- and Medium-Scale TEC Spatial Variations and Irregularities from Ground-Based GNSS Observations

Xiaoqing Pi, Shadi Oveisgharan, Ekaterina Tymofyeyeva, Heresh Fattahi, Paul Rosen, and Vardan Akopian
Jet Propulsion Laboratory, California Institute of Technology, Pasadena, CA, USA

BIOGRAPHIES

Dr. Xiaoqing Pi joined NASA's Jet Propulsion Laboratory, California Institute of Technology, in 1996. His primary research interests include ionospheric remote sensing and modeling. He has led and conducted NASA's research projects for imaging the ionosphere and ionospheric irregularities using GNSS and synthetic aperture radar, and for developing an ionospheric multimodel ensemble prediction system. He has co-developed the rate of TEC index (ROTI), Global Assimilative Ionospheric Model (GAIM), and Global Maps of Ionospheric Irregularities (GMIIS).

Shadi Oveisgharan was born in Isfahan, Iran. She received the B.Sc. degree from the Sharif University of Technology, Tehran, and the M.S. degree from the University of Michigan, Ann Arbor, MI, both in electrical engineering, and the Ph.D. degree in electrical engineering from Stanford University, Stanford, CA. She is currently serving as the science performance tool lead for phase I of the SDC mission. She was awarded NASA Postdoctoral Program (NPP) in 2007. She joined JPL as a Scientist in 2010 and was involved in many different projects and missions including NISAR and SMAP missions. Her current research interests include InSAR radar remote sensing application and modeling electromagnetic scattering in snow and vegetation.

Ekaterina Tymofyeyeva received her B.S. degree in physics from The College of New Jersey in 2009, and a Ph.D. in earth science from the University of California, San Diego in 2018. Her research interests include using Interferometric Synthetic Aperture Radar (InSAR) and Global Positioning System (GPS) measurements of crustal deformation to further the understanding of the earthquake cycle. Dr. Tymofyeyeva is currently working with the NASA-ISRO Synthetic Aperture Radar (NISAR) Algorithm Development Team at the Jet Propulsion Laboratory (JPL), California Institute of Technology (CalTech) in Pasadena. She is also serving as a Deputy Program Applications Co-lead for the NISAR mission, and the Secretary of the WInSAR Executive Committee.

Heresh Fattahi is a member of the Synthetic Aperture Radar (SAR) Algorithms and Processing group at the NASA's Jet Propulsion Laboratory. His research interests include algorithm development for SAR, Interferometry SAR (InSAR) and InSAR time-series analysis and uncertainty quantification of SAR-derived measurements. He is currently leading the algorithm development for Level-2 products from NASA-ISRO SAR (NISAR) mission. He has developed algorithms to estimate and correct ionospheric phase effects from stacks of SAR data and is currently working on understanding the spatio-temporal characteristics of ionospheric TEC and TEC gradients and their impact on the low-frequency SAR sensors.

Paul A. Rosen received a PhD in Electrical Engineering from Stanford University and his M.S. and B.S in Electrical Engineering from University of Pennsylvania. He is currently Project Scientist for NASAISRO synthetic aperture radar mission (NISAR) at the Jet Propulsion Laboratory, California Institute of Technology (Caltech). He is also the study coordinator for NASA's Surface Deformation and Change Decadal Survey Architecture Study. His assignments at JPL have encompassed scientific and engineering research and development of radar instruments and applications, as well as technical, organizational and programmatic management of radar developments at JPL. Dr. Rosen is a visiting faculty member at the Division of Geological and Planetary Sciences at Caltech, and has authored on over 40 journal and book chapter publications, and over 100 conference papers. He currently serves as the IEEE Geoscience and Remote Sensing Society Director for Global Activities.

Vardan Akopian received his B.S. degree in mathematics from Yerevan State University and his M.A. and Ph.D. degrees in applied mathematics from University of Southern California. He joined JPL in 2003 and worked on the Global Assimilative Ionospheric Modeling (GAIM) project. He is currently a researcher at JPL and a senior software engineer at Google.

https://doi.org/10.33012/2021.17856

ABSTRACT

This paper describes approaches to measuring small- and medium-scale spatial rate of vertical TEC from GNSS observations. The horizontal scale size measured by small-scale TEC spatial rate (STSR, in TECU/km), including its latitude and longitude components, ranges from about 1.8 km to 15 km at 450 km altitude. The medium-scale TEC gradient components can be derived from global ionospheric map (GIM) based TEC gradient (GBTG) over about 110 km horizontally at low and middle latitudes, with smaller scale lengths in the longitude component in the polar region. Our analyses of GPS data show that the latitude component of STSR and GBTG is much larger than the longitude component. The spatial rates in most regions of the globe are relatively small, and their absolute mean values are mostly under 0.03 TECU/km. However, STSR is substantially larger, often greater than 0.05 TECU/km, in the equatorial ionospheric anomaly (EIA) region than in other regions, or when ionospheric disturbances occur. The disturbances include ionospheric irregularities, significant changes of regional ionospheric state during space weather events, and traveling ionospheric disturbances. Combined global TEC spatial rate (CGTR) (also named combined global TEC gradient, CGTG) with STSR and GBTG is also shown in this paper as snapshots using data from networks of more than three thousand GNSS receivers. The comparisons between the mean STSR and GBTG in each bin indicate that their regional variation patterns are consistent though there are subtle differences between them particularly in the equatorial anomaly region or during ionospheric disturbances particularly during space weather events. The difference is at least partially attributed to the fact that the GBTG smooths out small-scale variations particularly in regions where spatial variations are large.

1. INTRODUCTION

TEC spatial variations cause horizontal changes of signal delay and phase advance in trans-ionospheric radio signals at VHF through L band. The effect can contaminate along- and cross-track signal phase measurements of spaceborne synthetic aperture radar carried by Earth remote sensing satellites. It is also a concern to satellite- and ground-based augmentation systems if the variations become large at small distances. Measuring the TEC effect can help estimate and minimize distortions of the data generated by these systems. In remote sensing mission designs, a demand to estimate TEC spatial difference in short distance globally is often raised. Although TEC data can be derived from GNSS observations from many thousand GNSS tracking stations around globe, the distribution of measurements in many regions and local areas are still very sparse. This hinders approaches such as planar or surface fit, which requires a substantial number of data samples in small areas (~tens to a few hundred km^2).

This paper describes a method to derive small-scale (2 to 15 km) TEC spatial rate (STSR) measured in TEC units (1 TECU = 10^{16} electrons/m^2) per kilometer, or TECU/km. The STSR measurements are based on GNSS phase and pseudorange observed using ground-based geodetic type dual-frequency or multiband GNSS receivers. In addition, we will also describe global ionospheric map (GIM) based TEC gradient (GBTG) that measures TEC spatial changes sampled at medium-scales (~100 km).

Compared with STSR, the temporal Rate of TEC Index (ROTI) has already been developed in the past based on GNSS dual-frequency phase data [1][2]. In that approach ROTI is defined as the standard deviation of detrended TEC temporal fluctuations within a time interval (typically 5 minutes). The index characterizes ionospheric irregularities and has been widely used in studies of ionospheric irregularities and scintillation.

2. SMALL-SCALE TEC SPATIAL RATE

In this approach, small-scale TEC spatial rate (STSR) is computed using the difference of vertical TEC measured between adjacent data samples along same receiver-satellite track at typical 30-second intervals. Vertical TEC data can be derived following three steps: (1) processing dual-frequency signal phase and pseudorange data to derived relative line-of-sight TEC; (2) removing satellite and receiver instrument interfrequency biases; (3) converting bias-removed line-of-sight TEC to vertical TEC. Such GNSS-TEC data processing has been performed at the Jet Propulsion Laboratory and a few other research centers to generate ionospheric products including global ionospheric map (GIM) [3][4]. In our STSR processing for spaceborne radar mission designed, measurements are needed from thousands of globally distributed receivers. This requires an additional step to remove many additional receiver biases following equations (1) and (2) as follows:

$$\mathbf{STEC_{obs}} = \mathbf{M\ VTEC} + \boldsymbol{b_s} + \boldsymbol{b_r} \tag{1}$$

or

$$\boldsymbol{b_r} = \mathbf{STEC_{obs}} - \mathbf{M\ VTEC} - \boldsymbol{b_s}\ , \tag{2}$$

where $STEC_{obs}$ is slant TEC observation, M is the vertical to slant mapping function which depends on the observation elevation angle, VTEC is bias-removed vertical TEC, b_s and b_r are satellite and receiver instrument interfrequency biases, respectively. In our approach, VTEC and satellite biases from JPL's GIM are used to estimate all additional receiver biases. This technique has been used in processing GPS data from a large number of GNSS receiver stations [5].

No cross-track data are used to compute STSR in order to avoid possible bias estimation errors and to reduce possible different data noise on different receiver platforms. The spacing for 30-second sampled GPS observations along a same receiver-to-satellite track ranges approximately from 1.8 km to 15 km depending on observation elevation angle. This range falls into the domain of small scales. With such data, STSR and its latitude and longitude modulations or components are defined as follows:

$$\mathrm{STSR} = d\mathrm{TEC}/dS, \tag{3}$$
$$\mathrm{STSR}_\theta = d\mathrm{TEC}\sin(\gamma)/dS, \tag{4}$$
$$\mathrm{STSR}_\varphi = \mathrm{dTEC}\cos(\gamma)/dS, \tag{5}$$

where dTEC is the TEC difference between adjacent data samples along the same receiver-satellite track, dS is the horizontal distance at 450 km altitude between the two positions of the data samples, and γ is defined as the angle determined by the arc lengths in latitude and longitude directions between the two data samples, i.e.,

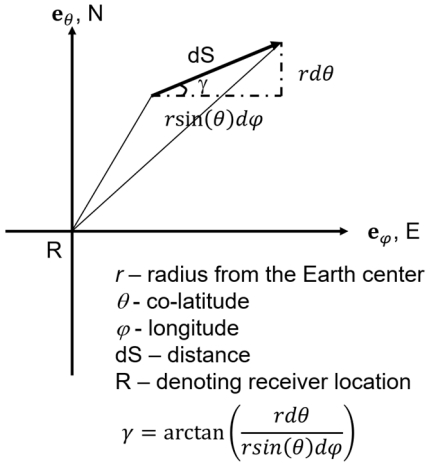

Figure 1. Schematic of observation geometry for measuring small-scale TEC spatial rate (STSR).

$$\gamma = \arctan\left(\frac{rd\theta}{rsin(\theta)d\varphi}\right) \tag{6}$$

where r is the radius from the Earth center to 450 km altitude, θ and φ are co-latitude and longitude of the observation, respectively. Figure 1 gives a schematic of the related geometry. Equations (4) and (5) can also be explained as the decomposition of dTEC/dS to latitude and longitude components. With STSR and its components so defined, dTEC in any direction can be estimated with observation geometry of a concerned satellite mission. Figures 2 and 3 show an example of GPS observations obtained using a receiver in Japan's GEONET, and STSR measurements derived from the data.

Several properties of the STSR approach are as follows: (1) dTEC/dS normalizes TEC changes with distance; (2) measuring dTEC exclusively along the same receiver-satellite track helps to reduce possible bias estimation errors for different receivers or satellites; (3) the decomposition to the latitude and longitude components helps to characterize TEC changes in different directions; (4) dTEC can be estimated from STSR with observation geometry for space mission designs. One disadvantage is that measurements taken consecutively for a certain time interval involve also TEC temporal variations. Hence this approach is valid when TEC temporal variations are small within short time intervals. When ionospheric irregularities or traveling ionospheric disturbances (TIDs) are present, STSR cannot be interpreted as spatial variation only. However, STSR under such scenarios can be used to detect these disturbances.

STSR measurements can be binned to obtain mean, root-mean-squares, and standard deviation over local areas and regions with a number of data samples in each bin. Figures 4–8 give examples of data counts, mean and standard deviation of STSR components ($STSR_\theta$ and $STSR_\varphi$) over Japan in 0.5°×0.5° (longitude × latitude) grid pixels. The GPS data collected from ~1300 GEONET stations are processed to produce STSR measurements. Figures 4 and 5 show color-coded data counts and mean $STSR_\theta$ for each bin for 00:00-00:05 UTC interval. Figures 6 and 7 show mean values of $STSR_\theta$ and $STSR_\varphi$, respectively, for 13:00-13:05 UTC interval. Figure 8 shows the standard deviation of $STSR_\theta$ during the same 13:00-13:04 UTC interval. Comparisons between STSR for the two UTC intervals (Figures 5 and 6) suggest that the ionosphere is disturbed during 13:00-13:05 UTC. Examining details of Figures 6 and 7, one can see oscillation or wavelike perturbation patterns. These perturbations are attributed to traveling ionospheric disturbances (TIDs) that often observed in the Japan region in evening hours during summer [6]. Our ROTI measurements (not shown here) of ionospheric irregularities created using the same GEONET data confirm the disturbances.

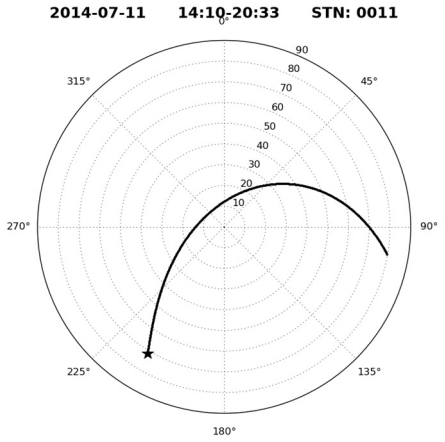

Figure 2. A ground observation track of GEONET receiver "0011" to satellite GPS26, displayed in observation azimuth and zenith angles from the receiver location (the center). The trajectory is projected from 450 km altitude that intercepts the line-of-sight radio links. The star symbol indicates the starting point.

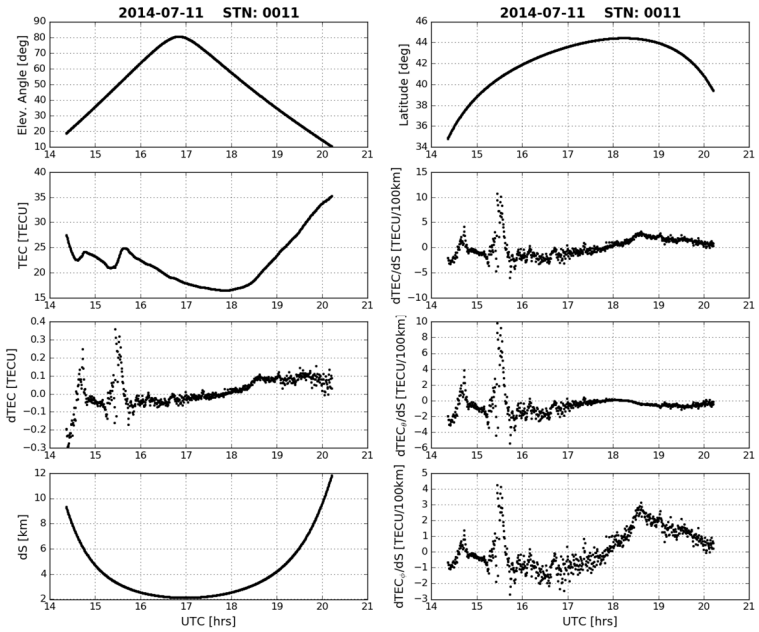

Figure 3. An example of TEC and STSR measurements made using GPS data from GEONET "0011" receiver tracking GPS26 satellite. Displayed are vertical TEC (2nd panel, left), dTEC (3rd panel, left), dS (bottom, left), and dTEC/dS (2nd panel, right) as well as its latitude and longitude components dTECsin(γ)/dS (3rd panel, right) and dTECcos(γ)/dS (bottom, right) with observation elevation angle and latitude in UTC sequence.

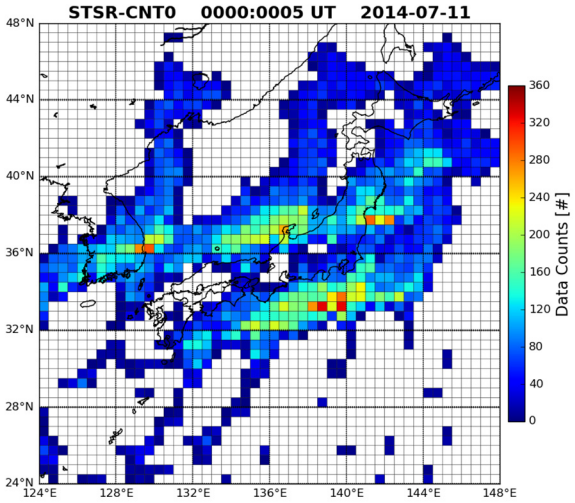

Figure 4. Data counts in 0.5°×0.5° (longitude × latitude) bins for STSR measurements using GEONET GNSS data

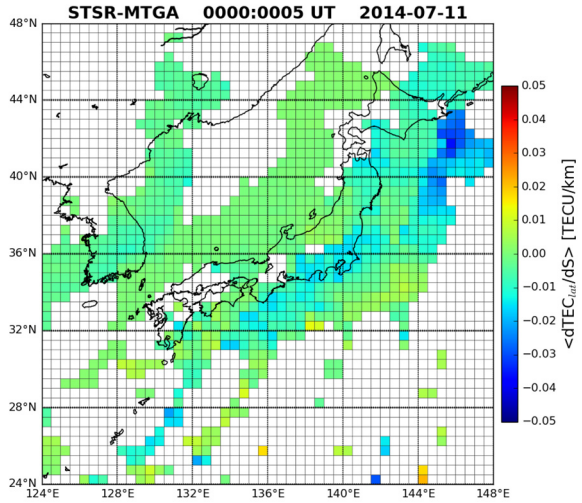

Figure 5. Mean $STSR_{\theta}$ derived from GEONET GPS data during 00:00-00:05 UTC on 11 July 2015.

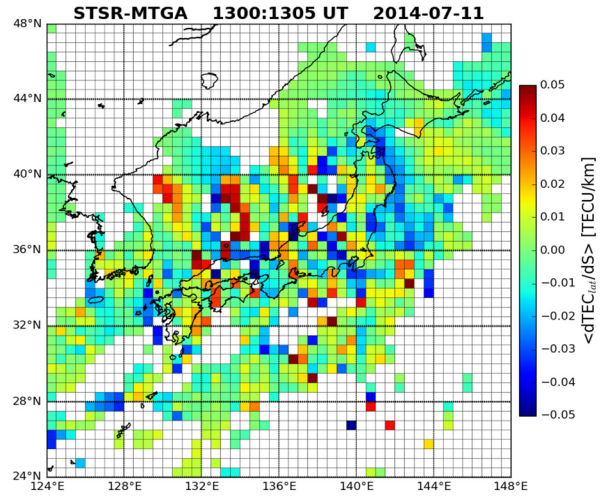

Figure 6. Mean STSR$_\theta$ derived from GEONET GPS data during 13:00-13:05 UTC on 11 July 2015.

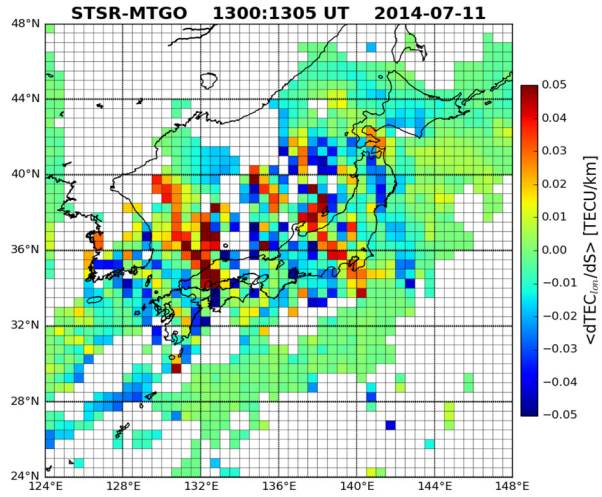

Figure 7. Standard deviation of STSR$_\varphi$ derived from GEONET GPS data during 13:00-13:05 UTC on 11 July 2015.

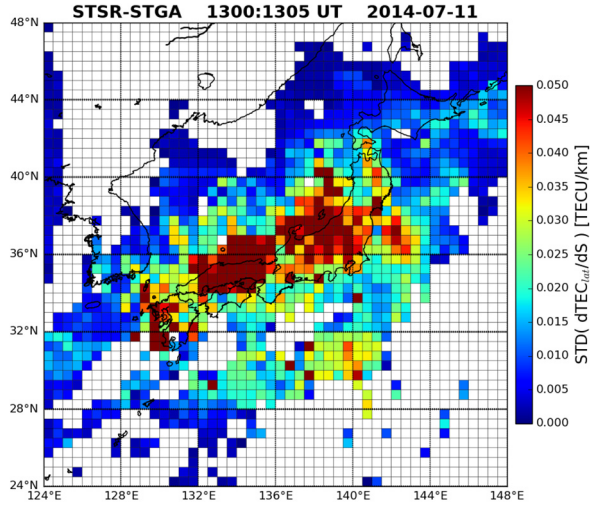

Figure 8. Standard deviation of STSR$_\theta$ derived from GEONET GPS data during 13:00-13:05 UTC on 11 July 2015.

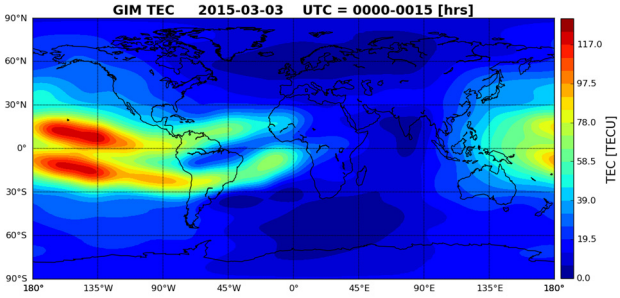

Figure 9. Global ionospheric TEC map (GIM) generated at JPL using globally distributed GPS data for 00:15 UTC 3 March 2015.

3. GIM-BASED TEC GRADIENT (GBTG) FOR MEDIUM-SCALE TEC CHANGES

With GIM generated using GNSS data distributed globally, shown in Figure 9 as an example, GBTG latitude and longitude components can be computed following the standard spherical gradient algorithm, i.e.,

$$\nabla \mathrm{TEC}(\theta,\varphi) = \frac{\partial \mathrm{TEC}}{r\partial\theta}\mathbf{e}_\theta + \frac{\partial \mathrm{TEC}}{r\sin(\theta)\partial\varphi}\mathbf{e}_\varphi. \qquad (7)$$

Figures 10-11 show the latitude and longitude component of TEC gradient computed using GIM with spatial resolutions of 1°×1° (longitude × latitude) and r at 450 km altitude for a 15-min UTC interval. It is noticed that in general the magnitude and variations of ∇_θTEC are much larger than ∇_φTEC at low latitudes. This is understandable given ionospheric TEC structure shown in Figure 9.

One of the issues of global 1°×1° grid is that arc length of the grid in longitude direction becomes smaller at higher latitudes. This would result in reduced data samples in the data bins in the polar region. One way to overcome this is to increase the grid size in the polar region. This will be done in updated GBTG, and also STSR as well as combined global TEC spatial rate (CGTR), also named combined global TEC gradient (CGTG) described below.

4. COMBINED GLOBAL TEC RATE (CGTR)

For a satellite mission, TEC changes in short distance along its orbit can be estimated using a combination of STSR and GBTG. One can use the mean value of either STSR$_\theta$ or STSR$_\varphi$ in an area (data bin) to estimate dTEC with observation

geometry, or to project GBTG to the concerned direction along the path. It should be pointed out that the global TEC mapping technique may smooth out actual small- and medium-scale structures. Figures 12-14 give examples of data counts in global bins gridded with 3.75°×2.5° (longitude and latitude) spacings and mean $STSR_\theta$ and $STSR_\varphi$ for each bin, respectively. An example of combined global TEC spatial rate (CGTR, also named combined global TEC gradient – CGTG) is shown in Figures 15-16. It shows mean values of CGTG components for the same bins with either STSR if data are available or GBTG. Compare these two spatial rates, we notice that there their general patterns are consistent, but there are differences between them at low and high latitudes. Some of these differences are attributed to the fact that global TEC mapping may smooth out small-scale TEC changes in regions where the ionospheric is more structured.

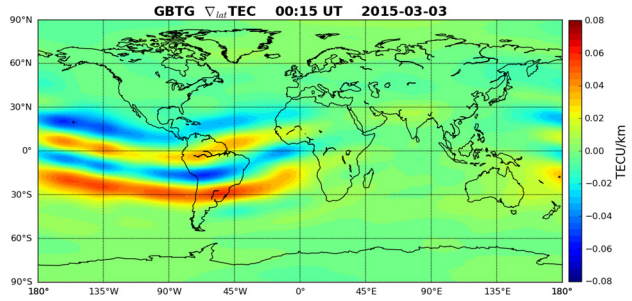

Figure 10. Global ∇_θTEC computed from GIM for 00:15 UTC 3 March 2015.

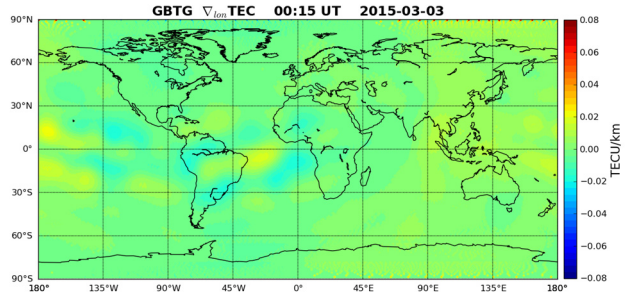

Figure 11. Global ∇_φTEC computed from GIM for 00:15 UTC 3 March 2015.

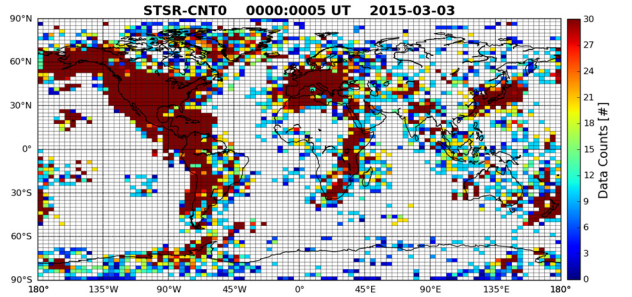

Figure 12. Data counts in 3.75°×2.5° (longitude × latitude) bins for mean STSR measurements obtained using globally distributed GPS data during 00:00-00:05 UTC on 3-March 2015.

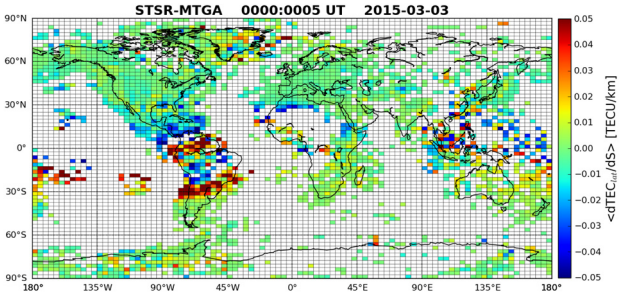

Figure 13. Mean $STSR_\theta$ in 3.75°×2.5° (longitude × latitude) bins obtained using globally distributed GPS data during 00:00-00:05 UTC on 3-March 2015.

5. TEC SPATIAL RATE DURING A SPACE WEATHER EVENT

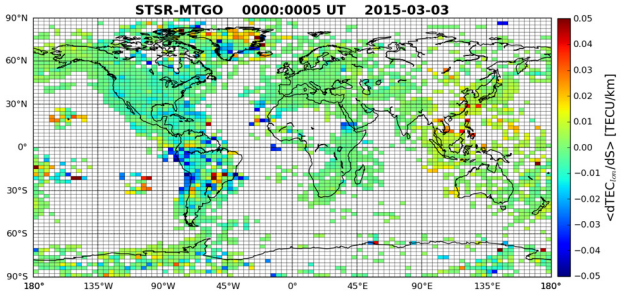

Figure 14. Mean $STSR_\varphi$ in 3.75°×2.5° (longitude × latitude) bins obtained using globally distributed GNSS data during 00:00-00:05 UTC on 3-March 2015.

The ionosphere can be disturbed during space weather events. When such events occur, charged particle precipitation from the magnetosphere, ionospheric electrodynamical perturbations and global thermospheric circulation changes can cause redistribution of ionospheric densities and significant changes in TEC and TEC gradient in different regions. Figures 17 and 18 show $CGTG_\theta$ and $CGTG_\varphi$ during 16:30-16:35 UTC on 17 March 2015 when the largest geomagnetic storm in solar cycle 24 (from Dec 2008 to Sep 2020) occurred during the day and the next day. During this interval, STSR and GBTG varies dramatically in many local areas and regions as well as on global scale compared with quiet times, such as those shown in data during 3 March 2015 (Figures 15 and 16). The significant changes are present in both latitude and longitude components.

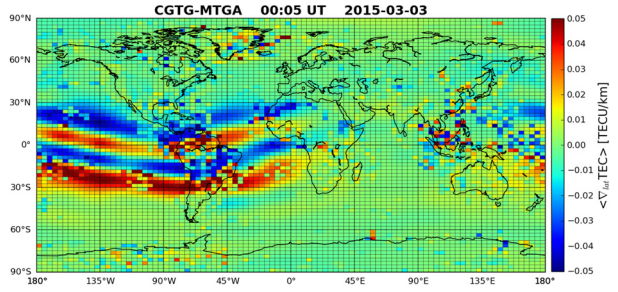

Figure 15. Mean CGTG$_\theta$ in 3.75°×2.5° (longitude × latitude) bins obtained using globally distributed GNSS data during 00:00-00:05 UTC on 3-March 2015.

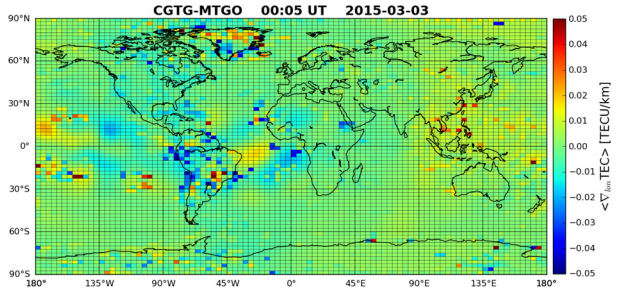

Figure 16. Mean CGTG$_\varphi$ in 3.75°×2.5° (longitude × latitude) bins obtained using globally distributed GNSS data during 00:00-00:05 UTC on 3-March 2015.

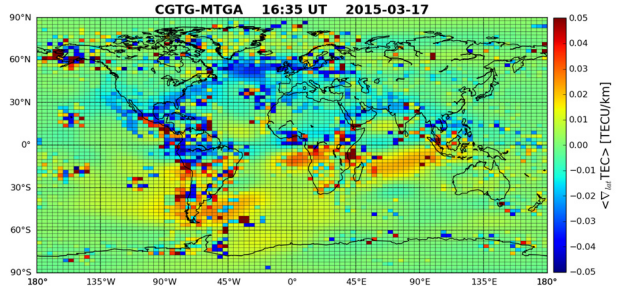

Figure 17. Mean CGTG$_\theta$ in 3.75°×2.5° (longitude × latitude) bins obtained using globally distributed GPS data during 16:30-16:35 UTC on 17-March 2015.

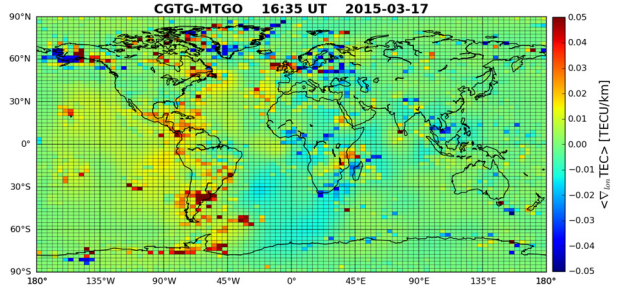

Figure 18. Mean CGTG$_\varphi$ in 3.75°×2.5° (longitude × latitude) bins obtained using globally distributed GPS data during 16:30-16:35 UTC on 17-March 2015.

6. CONCLUSIONS

A method is presented that can be used to measure latitude and longitude components of small-scale (1.8~15 km) TEC spatial rate (STSR) from GNSS observations for local areas and regions around the globe. With STSR, one can estimate TEC difference given observation geometry. Our analyses of GPS data show that STSR in most regions of the globe is relatively small, and its absolute mean value is mostly under 0.03 TECU/km. However, the value is substantially larger, often greater than 0.05 TECU/km, in the equatorial ionospheric anomaly (EIA) region than in other regions, or when ionospheric disturbances including TIDs and irregularities are present. The STSR approach is valid when TEC temporal variations are small within a time interval (5 minutes or shorter). When TIDs or ionospheric irregularities occur, the temporal variations may not be small. In these scenarios STSR can be used to detect and measure TIDs and ionospheric irregularities.

GIM-based TEC gradient (GBTG) measurements are also presented in this work, which is used to estimate medium-scale (~110 km) TEC changes globally. Comparisons of the magnitude between STSR and GBTG show that their regional variation patterns are consistent, but there are some differences in regions where the ionosphere presents large spatial variations such as the equatorial anomaly region or when ionospheric disturbances occur. In general, the GIM technique may smooth out the small-scale spatial variations particularly at low and higher latitudes. Our analyses of GPS data show that the latitude component of STSR and GBTG is much larger than the longitude component. It is demonstrated that the combined global TEC spatial rate (CGTR; also named combined global TEC gradient, CGTG) with STSR and GBTG allows us to estimate TEC changes in arbitrary directions for local areas and in regions around the globe using data from existing GNSS networks. The global grid for STSR, GBTG, and CGTG will be updated to increase the grid size in the longitude direction in the polar region. This will help to resolve the issue of reduced arc length in longitude direction and associated surface area, which affects the number of data samples for data bins in the polar region.

ACKNOWLEDGMENTS

The research conducted at the Jet Propulsion Laboratory, California Institute of Technology, is under a contract with the National Aeronautics and Space Administration. This work is partially supported by the Federal Aviation Administration

through the Wide Area Augmentation System program. The authors thank the GNSS CORS Division of Geospatial Information Authority of Japan (GSI) for providing GEONET data, and thank the International GNSS Service, National Geodetic Survey, UNAVCO, and Scripps Institute of Oceanography for making GNSS data available to research communities.

REFERENCES

1. Pi, X., A. J. Mannucci, U. J. Lindqwister, and C. M. Ho, Monitoring of global ionospheric irregularities using the worldwide GPS network, *Geophys. Research Letter*, *24*, 2283, 1997. https://doi.org/10.1029/97GL02273
2. Pi, X., A. J. Mannucci, B. Valant-Spaight, Y. Bar-Sever, L. J. Romans, S. Skone, L. Sparks, and G. M. Hall, Observations of global and regional ionospheric irregularities and scintillation using GNSS tracking networks, *Proceedings. ION GNSS Pacific PNT*, Honolulu, HI, April 2013.
3. A. J. Mannucci, B. D. Wilson, D. N. Yuan, C. H. Ho, U. J. Lindqwister, and T. F. Runge, A global mapping technique for GPS-derived ionospheric total electron content measurements, *Radio Science*, Vol. 33, No. 3, pp.565-582, May-June 1998. https://doi.org/10.1029/97RS02707
4. Iijima, B. A., I. L. Harris, C. M. Ho, U. J. Lindqwister, A. J. Mannucci, X. Pi, M. J. Reyes, L. C. Sparks, and B. D. Wilson (1999), Automated daily process for global ionospheric total electron content maps and satellite ocean altimeter ionospheric calibration based on Global Positioning System data, *Journal of Atmospheric and Solar-Terrestrial Physics*, 61, 1205–1218.
5. Komjathy, A., L. Sparks, B. D. Wilson, and A. J. Mannucci (2005), Automated daily processing of more than 1000 ground-based GPS receivers for studying intense ionospheric storms, *Radio Science*, 40, RS6006, doi:10.1029/2005RS003279.
6. Saito, A., Nishimura, M., Yamamoto, M. *et al.* Observations of traveling ionospheric disturbances and 3-m scale irregularities in the nighttime *F*-region ionosphere with the MU radar and a GPS network. *Earth, Planets and Space,* 54**,** 31–44 (2002). https://doi.org/10.1186/BF03352419